

# Raman Spectroscopy as an Indicator of Cu–S Bond Length in Type 1 and Type 2 Copper Cysteinate Proteins

Colin R. Andrew,<sup>1a</sup> Hyeyeong Yeom,<sup>1b</sup> Joan Selverstone Valentine,<sup>1b</sup>  
B. Göran Karlsson,<sup>1c</sup> Nicklas Bonander,<sup>1c</sup> Gertie van Pouderooyen,<sup>1d</sup>  
Gerard W. Canters,<sup>1d</sup> Thomas M. Loehr,<sup>1a</sup> and Joann Sanders-Loehr\*<sup>1a</sup>

Contribution from the Department of Chemistry, Biochemistry and Molecular Biology, Oregon Graduate Institute of Science & Technology, Portland, Oregon 97291-1000, Department of Chemistry and Biochemistry, University of California, Los Angeles, Los Angeles, California 90024, Department of Biochemistry and Biophysics, Chalmers University of Technology and Göteborg University, S-413 90 Göteborg, Sweden, and Leiden Institute of Chemistry, Gorlaeus Laboratories, 2300 RA Leiden, The Netherlands

Received June 13, 1994<sup>®</sup>

**Abstract:** A series of metalloprotein mutants with novel copper cysteinate coordination environments has been probed by resonance Raman (RR) spectroscopy. These include H117G, M121E, and M121K mutants of *Pseudomonas aeruginosa* azurin and H46C, H80C, and H120C mutants of yeast CuZn-superoxide dismutase. In each case, excitation within a (Cys)S → Cu charge transfer band leads to the enhancement of multiple vibrational modes of the copper cysteinate moiety. The predominant Cu–S stretching vibration,  $\nu(\text{Cu–S})$ , located in the 300–450  $\text{cm}^{-1}$  region, can be identified by (i) its large S- and Cu-isotope shifts, (ii) its high RR intensity, and (iii) its role as the generator of combination bands. The  $\nu(\text{Cu–S})$  frequency appears to be a sensitive indicator of Cu–S(Cys) bond strength and, hence, copper coordination geometry. In the case of type 1 (T1) sites, the increased influence of the weak axial ligand upon moving from a trigonal planar (axial EPR) toward a more tetrahedral (rhombic EPR) geometry is associated with a decrease in  $\nu(\text{Cu–S})$  from  $\sim 420$  to  $\sim 350$   $\text{cm}^{-1}$ . In the case of type 2 (T2) sites with four strong ligands,  $\nu(\text{Cu–S})$  undergoes further decreases from  $\sim 350$  to  $\sim 310$   $\text{cm}^{-1}$  as the geometry becomes more tetragonal. The Cu–S bond is successively weakened by trans ligand effects as the geometry approaches square planar. The decreased strength of the Cu–S(Cys) bond is further reflected in the increased strength of the adjacent S–C bond whose stretching frequency varies from  $\sim 750$   $\text{cm}^{-1}$  for axial T1 sites to  $\sim 765$   $\text{cm}^{-1}$  for T2 sites. The  $\sim 100\text{-cm}^{-1}$  range in  $\nu(\text{Cu–S})$  corresponds to a change in Cu–S(Cys) bond distance from  $\sim 2.13$  Å for an axial T1 site to  $\sim 2.29$  Å for a tetragonal T2 site. The overlap of T1 and T2  $\nu(\text{Cu–S})$  frequencies near 350  $\text{cm}^{-1}$  shows that both types of Cu site can have similar Cu–S(Cys) bond strengths, despite their different EPR and optical characteristics, and points to a continuum of geometries linked through a tetrahedral structure which we describe as a T1.5 intermediate Cu site.

## Introduction

The copper thiolate moiety, in which a Cu ion is ligated by a cysteine residue, occurs in a variety of proteins<sup>2</sup> and exhibits a surprisingly large range of coordination geometries (Figure 1). Type 1 (T1) copper thiolates function as electron-transfer catalysts in mononuclear and multinuclear copper proteins.<sup>3</sup> They are characterized by EPR spectra with unusually narrow hyperfine splitting ( $A_{\parallel} < 90 \times 10^{-4}$   $\text{cm}^{-1}$ ) and varying degrees of rhombicity.<sup>4,5</sup> Proteins with axial T1 EPR spectra have an intense blue color due to a (Cys)S → Cu CT absorption near 600 nm ( $\epsilon \approx 5000$   $\text{M}^{-1}$   $\text{cm}^{-1}$ ), together with a weak shoulder near 450 nm that also has significant S → Cu CT contribution.<sup>6</sup> Proteins with rhombic T1 EPR spectra have a greater proportion of their CT intensity in the 450-nm band which also gives them a more green appearance.<sup>6,7</sup>

In general, the X-ray crystal structures of axial T1 proteins<sup>8,9</sup> have revealed a short Cu–S(Cys) bond of  $2.12 \pm 0.05$  Å. This short bond is due to the trigonal array of three strong ligands

(His<sub>2</sub>Cys), with a weaker axial interaction (usually Met) at a distance of  $\sim 3$  Å (Figure 1A). In rhombic T1 sites such as pseudoazurin and nitrite reductase, X-ray crystal structures<sup>6,8</sup> reveal a tetrahedral distortion with the Cu  $\sim 0.4$  Å out of the His<sub>2</sub>Cys plane and closer to the axial ligand and with the Cu–S(Cys) bond lengthened to  $\sim 2.16$  Å (Figure 1B). An important question is whether the narrow hyperfine splitting of both axial and rhombic T1 sites is due to the short Cu–S(Cys) bond distance<sup>10</sup> or their overall geometry.<sup>11</sup> This issue is clouded by the uncertainty of Cu–S distances from X-ray crystallography as, for example, the report of a 2.25-Å Cu–S(Cys) distance in the crystal structure of *Pseudomonas aeruginosa* azurin.<sup>12</sup>

(6) (a) Han, J.; Loehr, T. M.; Lu, Y.; Valentine, J. S.; Averill, B. A.; Sanders-Loehr, J. *J. Am. Chem. Soc.* **1993**, *115*, 4256–4263. (b) Sanders-Loehr, J. In *Bioinorganic Chemistry of Copper*; Karlin, K. D., Tyeklar, Z., Eds.; Chapman & Hall: New York, 1993; pp 51–63.

(7) Lu, Y.; LaCroix, L. B.; Lowery, M. D.; Solomon, E. I.; Bender, C. J.; Peisach, J.; Roe, J. A.; Gralla, E.; Valentine, J. S. *J. Am. Chem. Soc.* **1993**, *115*, 5907–5918.

(8) Adman, E. T. *Adv. Protein Chem.* **1991**, *42*, 145–197.

(9) Han, J.; Adman, E. T.; Beppu, T.; Codd, R.; Freeman, H.; Huq, L.; Loehr, T. M.; Sanders-Loehr, J. *Biochemistry* **1991**, *30*, 10904–10913.

(10) Shadle, S. E.; Penner-Hahn, J. E.; Schugar, H. J.; Hedman, B.; Hodgson, K. O.; Solomon, E. I. *J. Am. Chem. Soc.* **1993**, *115*, 767–776.

(11) Addison, A. W. In *Copper Coordination Chemistry: Biochemical and Inorganic Perspectives*; Karlin, K. D., Zubieta, J., Eds.; Adenine Press: New York, 1983; pp 109–128.

(12) Nar, H.; Messerschmidt, A.; Huber, R.; van de Kamp, M.; Canters, G. W. *J. Mol. Biol.* **1991**, *221*, 765–772.

<sup>®</sup> Abstract published in *Advance ACS Abstracts*, November 15, 1994.

(1) (a) Oregon Graduate Institute of Science & Technology. (b) University of California, Los Angeles. (c) Chalmers University of Technology and University of Göteborg. (d) Gorlaeus Laboratories.

(2) Canters, G. W.; Gilardi, G. *FEBS Lett.* **1993**, *325*, 39–48.

(3) Sykes, A. G. *Adv. Inorg. Chem.* **1991**, *36*, 377–408.

(4) Adman, E. T. In *Metalloproteins*; Harrison, P., Ed.; Verlag Chemie: Weinheim, FRG, 1985; Part I, pp 1–42.

(5) Solomon, E. I.; Baldwin, M. J.; Lowery, M. D. *Chem. Rev.* **1992**, *92*, 521–542.

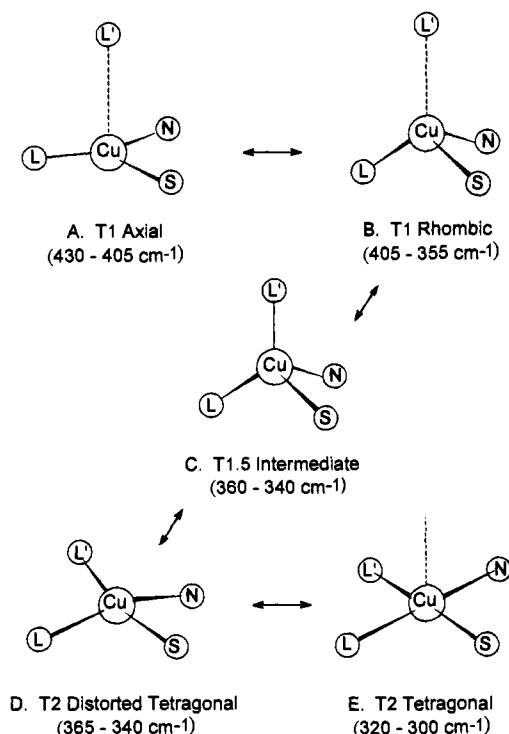


**Figure 1.** Coordination geometries of copper sites in copper cysteinate proteins. The scheme shows ligand movements required for interconversion between different geometries and range of RR frequencies for the Cu–S(Cys) stretch. In wild-type azurin (T1 axial), S = C112, N = H46, L = H117, and L' = M121. In H117G(His) mutant azurin (T2 tetragonal) the probable ligands are S = C112, N = H46, and L, L' = imidazole and amino groups of exogenous histidine. In wild-type Cu<sub>2</sub>-Zn<sub>2</sub>-SOD, the Cu site (T2 tetragonal) has 4 N ligands (H46, H48, H63, and H120) with H63 bridging to a neighboring Zn. In the H80C (green) mutant of SOD with Cu (T1 rhombic) in place of Zn, the probable ligands are S = C80, N = H71, and L, L' = D83, H63.

Resonance Raman (RR) spectroscopy is another method for determining Cu–S(Cys) bond distances. In contrast to UV–vis and EPR spectra which reflect overall Cu coordination geometry, RR spectra primarily provide information on the copper cysteinate moiety.<sup>6,13,14</sup> Excitation within (Cys)S → Cu(II) CT bands leads to the enhancement of five or more vibrational fundamentals between 350 and 500 cm<sup>-1</sup>. These are believed to originate from kinematic and vibronic coupling of the Cu–S(Cys) stretch,  $\nu(\text{Cu}-\text{S})$ , with internal ligand deformations,  $\delta(\text{Cys})$ , of the coplanar cysteine S $\gamma$ –C $\beta$ –C $\alpha$ –N moiety.<sup>9</sup> The RR band with the greatest Cu–S(Cys) stretching character can be identified by its large frequency shift upon S-isotope substitution, its high intensity, and its role as the generator of combination bands.<sup>15,16</sup> Thus, RR spectroscopy can be a sensitive indicator of the relative Cu–S(Cys) bond length, detecting differences that are within the  $\pm 0.07$ -Å error limit<sup>17</sup> of protein X-ray crystallography.

Proteins containing *type 2* (T2) copper cysteinates are distinguished from their T1 counterparts by a higher value of

$A_{11}$  ( $>90 \times 10^{-4} \text{ cm}^{-1}$ ) and a shift of the most intense absorption band to  $\sim 400 \text{ nm}$ , resulting in a yellow to orange color.<sup>2,6,18</sup> In contrast to T1 proteins, the only X-ray structural data available at present for T2 copper thiolates are for model complexes.<sup>19</sup> The main structural difference from T1 sites appears to be a more nearly tetragonal arrangement with four strong ligands approximating a square plane (Figure 1E) as, for example, in the Cu[SCH<sub>2</sub>CH(CO<sub>2</sub>CH<sub>3</sub>)NHCH<sub>2</sub>]<sub>2</sub> model complex with two thiolato and two amino ligands.<sup>20</sup> The presence of the fourth strong ligand accounts for the increase in Cu–S bond length to 2.25–2.36 Å.<sup>19</sup> Studies on another T2 model complex, Cu(imino)<sub>2</sub>(S-pyrazole)<sub>2</sub> doped into tetrahedral Zn(imino)<sub>2</sub>(S-pyrazole)<sub>2</sub>,<sup>21</sup> have demonstrated that the resultant tetrahedral distortion causes the EPR  $A_{11}$  value to decrease from 137 to  $118 \times 10^{-4} \text{ cm}^{-1}$ , a value approaching that of a T1 site. Such a tetrahedral distortion can occur by a twist of the two opposing X–Cu–Y ligand planes of a tetragon (Figure 1E) to yield a distorted tetragon (Figure 1D). In this view, a tetrahedron is actually part of a continuum of structures,<sup>22</sup> and the geometries of T1 and T2 Cu are conveniently described as arising from different distortions of a T1.5 intermediate (Figure 1C).

The primary goal of the present study was to use RR spectroscopy to investigate differences in the Cu–S(Cys) bond lengths in T1 and T2 copper cysteinate sites. This was facilitated by the availability of Cu-ligand mutants, for which the following assignments can be made on the basis of our studies. Wild-type azurin from *P. aeruginosa*<sup>12</sup> is found to have an axial T1 Cu site (Figure 1A), whereas the H117G mutant with bidentate exogenous ligands<sup>16,23</sup> has a tetragonal T2 site (Figure 1E). In contrast, the M121E and M121K mutants<sup>24</sup> of *P. aeruginosa* azurin at neutral pH have an intermediate T1.5 site (Figure 1C). For CuZn-superoxide dismutase (SOD) from *Saccharomyces cerevisiae*,<sup>25</sup> insertion of a Cys ligand (H80C) and a Cu into the Zn site creates a transient yellow,<sup>26</sup> tetragonal T2 site (Figure 1D) followed by a stable green,<sup>6,7</sup> rhombic T1 site (Figure 1B). Insertion of a Cys ligand (H46C or H120C) into the Cu site<sup>6,18</sup> creates additional examples of distorted tetragonal T2 sites (Figure 1D).

Results from the present RR study show that all of the above mutants exhibit 4–12 resonance-enhanced vibrations between 250 and 500 cm<sup>-1</sup>. The appearance of a set of coupled [ $\nu(\text{Cu}-\text{S}) + \delta(\text{Cys})$ ] modes is thus typical of copper cysteinate coordination in proteins, regardless of the Cu-site geometry. Sulfur-isotope substitution reveals that in each case the greatest RR intensity is correlated with the greatest Cu–S(Cys) stretching character, thereby making it possible to use this mode as an indicator of Cu–S bond length. The major difference for

(18) (a) Lu, Y.; Gralla, E. B.; Roe, J. A.; Valentine, J. S. *J. Am. Chem. Soc.* **1992**, *114*, 3560–3562. (b) Yeom, H. Ph.D. Dissertation, University of California, Los Angeles, 1993.

(19) Kitajima, N. *Adv. Inorg. Chem.* **1993**, *39*, 1–77.

(20) Bharadwaj, P. K.; Potenza, J. A.; Schugar, H. J. *J. Am. Chem. Soc.* **1986**, *108*, 1351–1352.

(21) (a) Toftlund, H.; Becher, J. In *Biological & Inorganic Copper Chemistry*; Karlin, K. D., Zubieta, J., Eds.; Adenine Press: New York, 1985; pp 231–236. (b) Anderson, O. P.; Becher, J.; Frydendahl, H.; Taylor, L. F.; Toftlund, H. *J. Chem. Soc., Chem. Commun.* **1986**, 699–701.

(22) Zabrodsky, H.; Peleg, S.; Avnir, D. *J. Am. Chem. Soc.* **1993**, *115*, 8278–8289.

(23) den Blaauwen, T.; Canters, G. W. *J. Am. Chem. Soc.* **1993**, *115*, 1121–1129.

(24) (a) Karlsson, B. G.; Nordling, M.; Pascher, T.; Tsai, L.-C.; Sjölin, L.; Lundberg, L. G. *Protein Eng.* **1991**, *4*, 343–349. (b) Pascher, T.; Karlsson, G.; Nordling, M.; Malmström, B. G.; Vänngård, T. *Eur. J. Biochem.* **1993**, *212*, 289–296. (c) Murphy, L. M.; Karlsson, B. G.; Hasnain, S. S., personal communication.

(25) (a) Getzoff, E. D.; Tainer, J. A.; Weiner, P. K.; Kollman, P. A.; Richardson, J. S.; Richardson, D. C. *Nature (London)* **1983**, *306*, 287–290. (b) Valentine, J. S.; Pantoliano, M. W. In *Copper Proteins*; Spiro, T. G., Ed.; Wiley: New York, 1981; pp 291–357.

(26) Yeom, H.; Lu, Y.; Andrew, C. R.; Sanders-Loehr, J.; Valentine, J. S., manuscript in preparation.

(13) Nestor, L.; Larrabee, J. A.; Woolery, G.; Reinhammar, B.; Spiro, T. G. *Biochemistry* **1984**, *23*, 1084–1093.

(14) (a) Blair, D. F.; Campbell, G. W.; Schoonover, J. R.; Chan, S. I.; Gray, H. B.; Malmström, B. G.; Pecht, I.; Swanson, B. I.; Woodruff, W. H.; Cho, W. K.; English, A. M.; Fry, A. F.; Lum, V.; Norton, K. A. *J. Am. Chem. Soc.* **1985**, *107*, 5755–5766. (b) Woodruff, W. H.; Dyer, R. B.; Schoonover, J. R. In *Biological Applications of Raman Spectroscopy*; Spiro, T. G., Ed.; John Wiley: New York, 1988; Vol. 3, pp 413–438.

(15) Dave, B. C.; Germanas, J. P.; Czernuszewicz, R. S. *J. Am. Chem. Soc.* **1993**, *115*, 12175–12176.

(16) den Blaauwen, T.; Canters, G. W.; Hoitink, C. W. G.; Han, J.; Loehr, T. M.; Sanders-Loehr, J. *Biochemistry* **1993**, *32*, 12455–12464.

(17) Guss, J. M.; Bartunik, H. D.; Freeman, H. C. *Acta Crystallogr. B* **1992**, *48*, 790–811.

T2 proteins is that the most intense RR feature is shifted to lower energy by 50–100  $\text{cm}^{-1}$ . All of the T2 mutants examined had their major  $\nu(\text{Cu-S})$  mode between 317 and 366  $\text{cm}^{-1}$ , indicating a longer Cu-S(Cys) bond than in axial T1 Cu sites where the predominant  $\nu(\text{Cu-S})$  mode is  $>400 \text{ cm}^{-1}$ . However, some of the tetragonal T2 sites have similar Cu-S(Cys) bond strengths to highly rhombic T1 sites, both exhibiting  $\nu(\text{Cu-S})$  values close to 360  $\text{cm}^{-1}$ . Thus, the different EPR parameters which distinguish T1 and T2 sites appear to derive largely from the *Cu-site geometry* and not the Cu-S(Cys) bond length.

## Experimental Procedures

**Protein Samples.** The azurin-M121E and M121K mutants from *Pseudomonas aeruginosa* were obtained by cassette mutagenesis from a cloned *azu* gene expressed in *Escherichia coli* as described previously.<sup>24a</sup> The azurin-H117G mutant from *P. aeruginosa* was expressed in *E. coli* and purified as described.<sup>27</sup> For azurin-H117G fully substituted with <sup>34</sup>S, cells were grown on minimal medium containing 1 mL/L of a trace element solution,<sup>28</sup> 1 mM  $\text{Na}_2^{34}\text{SO}_4$  (90 atom %, ICON), and 0.14 mM ampicillin and induced with 0.1 mM IPTG. The imidazole and histidine adducts of azurin-H117G were prepared as described,<sup>16</sup> and the samples were concentrated in a Microcon-10 ultrafiltration device (Amicon).

The CuZn-superoxide dismutase mutants (H46C, H120C, and H80C) from *Saccharomyces cerevisiae* were expressed in *E. coli* and prepared in the apo form.<sup>7,18</sup> In the case of H80C-SOD, the protein was reconstituted with 4  $\text{Cu}^{2+}$  (in both the Cu and Zn sites) to yield the  $\text{Cu}_2\text{Cu}_2$  species. Freshly reconstituted H80C-SOD was frozen within 5 min to obtain the yellow T2 form or else left at room temperature for 24 h to convert to the green rhombic T1 species. The apo forms of H46C-SOD and H120C-SOD were equilibrated initially with 2  $\text{Zn}^{2+}$  overnight (4 °C) before adding 2  $\text{Cu}^{2+}$  to form the  $\text{Cu}_2\text{Zn}_2$  species. Finally, protein samples were concentrated by centrifugation in a Microcon-10 ultrafiltration device. Reported concentrations are per SOD subunit.

**Resonance Raman Spectroscopy.** Raman spectra were obtained on a modified Jarrell-Ash 25-300 spectrophotometer, equipped with an ORTEC Model 9302 amplifier/discriminator and an RCA C31034 photomultiplier, and interfaced to an Intel 310 computer. The desired excitation wavelengths were provided by the following lasers: Spectra-Physics 2025-11 Kr, Coherent Innova 90-6 Ar, and Coherent 599-01 dye (rhodamine 6G). Raman spectra were recorded at 0.5  $\text{cm}^{-1}/\text{s}$  in an  $\sim 150^\circ$  backscattering geometry from samples maintained at 15 K by use of a closed-cycle helium refrigerator (Air Products Displex).<sup>29</sup> Absolute frequencies are accurate to  $\pm 1 \text{ cm}^{-1}$ . Isotope shifts were obtained from spectra recorded under the identical experimental conditions and were evaluated by abscissa expansion and curve resolution of overlappings bands.<sup>29</sup> They are accurate to  $\pm 0.5 \text{ cm}^{-1}$ . For the excitation profiles, all spectra were recorded on the same sample, and enhancement was measured as the height of the protein chromophore peak relative to the height of the ice peak at 230  $\text{cm}^{-1}$ . The LabCalc or Grams 386 (Galactic Industries) programs were used for data analyses and Origin (MicroCal) was used for data presentation.

(27) den Blaauwen, T.; van de Kamp, M.; Canters, G. W. *J. Am. Chem. Soc.* **1991**, *113*, 5050–5052.

(28) Jeter, R. M.; Ingraham, J. L. *Arch. Microbiol.* **1984**, *138*, 124–130.

(29) Loehr, T. M.; Sanders-Loehr, J. *Methods Enzymol.* **1993**, *226*, 431–470.

(30) van Houwelingen, T.; Canters, G. W.; Stobbelaar, G.; Duine, J. A.; Frank Jzn, J.; Tsugita, A. *Eur. J. Biochem.* **1985**, *153*, 75–80.

(31) Husain, M.; Davidson, V. L. *J. Biol. Chem.* **1985**, *260*, 14626–14629.

(32) Sharma, K. D.; Loehr, T. M.; Sanders-Loehr, J.; Husain, M.; Davidson, V. L. *J. Biol. Chem.* **1988**, *263*, 3303–3306.

(33) Kitajima, N.; Fujisawa, K.; Tanaka, M.; Moro-oka, Y. *J. Am. Chem. Soc.* **1992**, *114*, 9232–9233.

(34) (a) Qiu, D.; Kilpatrick, L. T.; Kitajima, N.; Spiro, T. G. *J. Am. Chem. Soc.* **1994**, *116*, 2585–2590. (b) Qiu, D.; Spiro, T. G., personal communication.

(35) Ainscough, E. W.; Bingham, A. G.; Brodie, A. M.; Ellis, W. R.; Gray, H. B.; Loehr, T. M.; Plowman, J. E.; Norris, G. E.; Baker, E. N. *Biochemistry* **1987**, *26*, 71–82.

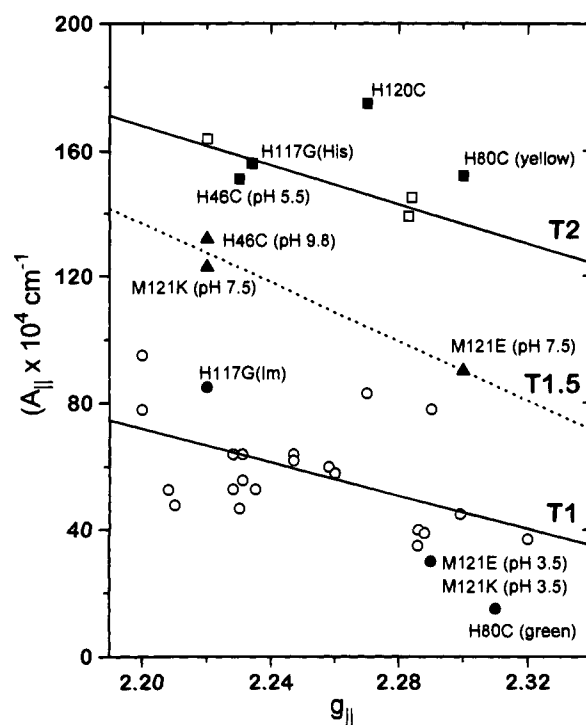


**Figure 2.** EPR parameters for copper cysteinate proteins. Linear correlations for T2 azurin-H117G mutants ( $\square$ ) based on 4 samples (from ref 23) and T1 proteins ( $\circ$ ) based on 21 samples (from ref 11). Individual points for T2 mutants ( $\blacksquare$ ), T1.5 mutants ( $\blacktriangle$ ), and T1 mutants ( $\bullet$ ) from data in Table 1.

## Results and Discussion

**Classification of Cu-Cys Mutants. (a) Type 1 Copper Sites.** T1 sites, whether axial (Figure 1A) or rhombic (Figure 1B), are typified by a trigonal  $\text{His}_2\text{Cys}$  donor set and a low EPR  $A_{||}$  value of  $<90 \times 10^{-4} \text{ cm}^{-1}$  (Table 1). A more accurate EPR classification is based on the consideration of both  $A_{||}$  and  $g_{||}$  parameters.<sup>11,39</sup> Such a compilation for a large number of T1 Cu proteins reveals the linear relationship shown by the lower line in Figure 2. In addition, all T1 sites exhibit an intense (Cys)S  $\rightarrow$  Cu(II) CT band ( $\lambda_2$ ) near 600 nm and a second (Cys)S  $\rightarrow$  Cu(II) CT band ( $\lambda_1$ ) near 460 nm (Table 1). The intensity ratio of the 460-nm band relative to the 600-nm band ( $\epsilon_1/\epsilon_2$ ) correlates with the extent of tetrahedral distortion (movement of the Cu away from the NNS plane of the  $\text{His}_2\text{Cys}$  ligand set and toward the axial ligand) and, thus, can be used as an indicator of the degree of T1 rhombicity.<sup>6,7</sup> Axial T1 sites (as in amicyanin and azurin) have  $\epsilon_1/\epsilon_2$  values  $\leq 0.12$ , whereas rhombic T1 sites (as in pseudoazurin) have  $\epsilon_1/\epsilon_2$  values  $\geq 0.20$  (Table 1).

The parameters in Table 1 enable us to classify a number of mutant copper cysteinate proteins. Azurin in which the equatorial His117 ligand has been converted to Gly binds exogenous imidazole to generate an axial T1 site nearly identical to that of wild-type azurin, but with an even smaller  $\epsilon_1/\epsilon_2$  value.<sup>16,23</sup> Substitution of the axial Met 121 ligand in azurin by Gln converts it into a rhombic T1 site with an  $\epsilon_1/\epsilon_2$  value of 0.20. The crystal structure of M121Q-azurin shows a movement of

(36) Romero, A.; Hoitink, C. W. G.; Nar, H.; Huber, R.; Messerschmidt, A.; Canters, G. W. *J. Mol. Biol.* **1993**, *229*, 1007–1021.

(37) Kakutani, T.; Watanabe, H.; Arima, K.; Beppu, T. *J. Biochem. (Tokyo)* **1981**, *89*, 463–472.

(38) Libby, E.; Averill, B. A. *Biochem. Biophys. Res. Commun.* **1992**, *187*, 1529–1535.

(39) (a) Peisach, J.; Blumberg, W. E. *Arch. Biochem. Biophys.* **1974**, *165*, 691–708. (b) Vännegård, T. In *Biological Applications of Electron Spin Resonance*, Schwartz, H. M., Bolton, J. R., Borg, D. C., Eds.; John Wiley: New York, 1972; pp 411–447.

**Table 1.** EPR, Adsorption and Raman Spectroscopic Properties of Copper(II) Thiolate Complexes

sample <sup>d</sup>	EPR (X-band) <sup>b</sup>		absorption (S → Cu CT) <sup>c</sup>			RR <sup>d</sup>			
	<i>g</i> <sub>  </sub>	<i>A</i> <sub>  </sub>	$\lambda_1$	$\lambda_2$	$\epsilon_1/\epsilon_2$	$\nu_i$	$\nu_e$	<i>I</i>	$\nu(\text{S}-\text{C})$
type 1 axial Cu site									
amicyanin <sup>e</sup>	2.24	52	464	<b>595</b>	0.11	430	430	500	756
Cu(pz) <sub>3</sub> (S- <i>t</i> Bu) <sup>f</sup>	2.21	70		<b>608</b>		437	437		
azurin <sup>g</sup>	2.26	60	460	<b>619</b>	0.11	408	408	~650	755
azurin-H117G (imidazole) <sup>h</sup>	2.22	85	460	<b>625</b>	0.04	406	406	~750	757
type 1 rhombic Cu site									
azurin-M121K (pH 3.5) <sup>i</sup>	2.29	30	440	<b>610</b>	0.29	407	407	~700	762
azurin-M121E (pH 3.5) <sup>j</sup>	2.29	30	440	<b>614</b>	0.20	370	399	~360	757
azurin-M121Q <sup>j</sup>	2.29	35	452	<b>610</b>	0.20	373	413	~360	761
pseudoazurin <sup>k</sup>		55	450	<b>593</b>	0.41	397	385	~130	773
nitrite reductase <sup>l</sup>	2.15	69	<b>458</b>	585	1.3	364	364	~200	
SOD-Cu <sub>2</sub> Cu <sub>2</sub> H80C (green) <sup>m</sup>	2.31	15	<b>459</b>	<b>595</b>	1.0	355	355	~150	
type 1.5 intermediate Cu site									
azurin-M121K (pH 7.5) <sup>i</sup>	2.22	123	<b>410</b>	530	2.7	358		~150	775
azurin-M121E (pH 7.5) <sup>j</sup>	2.30	90	<b>417</b>	570	1.8	343		~50	771
SOD-Cu <sub>2</sub> Zn <sub>2</sub> H46C (pH 9.8) <sup>n</sup>	2.22	132	<b>420</b>	530	2.7	357		~40	
type 2 tetragonal Cu site									
SOD-Cu <sub>2</sub> Zn <sub>2</sub> H46C (pH 5.5) <sup>n</sup>	2.23	151	<b>379</b>			342		~20	
SOD-Cu <sub>2</sub> Zn <sub>2</sub> H120C <sup>n</sup>	2.27	175	<b>406</b>			366		~15	
SOD-Cu <sub>2</sub> Cu <sub>2</sub> H80C (yellow) <sup>n</sup>	2.30	152	<b>411</b>	604	3.3	348		~40	
azurin-H117G (histidine) <sup>h</sup>	2.23	156	<b>400</b>			319		~70	763
azurin-H117G (H <sub>2</sub> O) <sup>n</sup>	2.28	139	<b>420</b>			317			768

<sup>a</sup> EPR and UV-vis data are from literature sources listed. Raman data are from this laboratory unless otherwise stated. <sup>b</sup> *A*<sub>||</sub> values in 10<sup>-4</sup> cm<sup>-1</sup>. <sup>c</sup>  $\lambda_{\text{max}}$  values in nm. Boldface numbers indicate the absorption peaks with the greatest intensity;  $\epsilon_1/\epsilon_2$  = ratio of extinction coefficients at  $\lambda_1$  and  $\lambda_2$ . <sup>d</sup>  $\nu$  in cm<sup>-1</sup>;  $\nu_i$  = frequency of the most intense peak;  $\nu_e$  = frequency of the fundamental that generates combination bands. *I* = molar intensity of strongest peak ( $\nu_i$ ) relative to that of the 980-cm<sup>-1</sup> sulfate peak using excitation close to  $\lambda_{\text{max}}$ . Approximate intensity (~) is expressed relative to the 230-cm<sup>-1</sup> ice mode and normalized to the sulfate value, based on liquid and frozen solution data for amicyanin (accuracy ±30%). <sup>e</sup> EPR for *Thiobacillus versutus* (ref 30), absorption and RR for *Paracoccus denitrificans* (refs 31 and 32). <sup>f</sup> Cu[HB(3,5-*i*Pr<sub>2</sub>pz)<sub>3</sub>](*tert*-butylthiolate) (ref 33), RR data (ref 34). <sup>g</sup> EPR and absorption for *Alcaligenes denitrificans* (ref 35), RR for *Pseudomonas aeruginosa* (refs 16 and 23). <sup>h</sup> *P. aeruginosa* (ref 24). <sup>i</sup> *A. denitrificans* (refs 16 and 36). <sup>k</sup> *Alcaligenes faecalis* S-6 (refs 9 and 37). <sup>l</sup> *Achromobacter cycloclastes* (refs 6 and 38). <sup>m</sup> *Saccharomyces cerevisiae* (refs 6 and 7). <sup>n</sup> *S. cerevisiae* (refs 18 and 26).

Cu away from the NNS plane and toward the axial Gln ligand.<sup>36</sup> This distortion toward a tetrahedral structure is even more marked for pseudoazurin<sup>40</sup> and nitrite reductase<sup>41</sup> where the Cu-S(Met) bond length has decreased to 2.76 and 2.62 Å, respectively, compared to 3.13 Å in wild-type azurin.<sup>35</sup> The  $\epsilon_1/\epsilon_2$  ratios have increased correspondingly to 0.41 for pseudoazurin and 1.3 for nitrite reductase (Table 1).

Several other species used in the present study can also be classified as having rhombic T1 Cu sites. The azurin mutants in which the axial Met121 ligand has been replaced by Lys or Glu have the requisite characteristics at pH 3.5, at which the new axial ligands are still protonated (Table 1). In addition to rhombic EPR signals and low *A*<sub>||</sub> values,<sup>24</sup> their  $\epsilon_1/\epsilon_2$  ratios of 0.29 and 0.20, respectively, are indicative of a small degree of tetrahedral distortion. Finally, the SOD mutant with Cys 80 in place of His in the tetrahedral Zn site exhibits a rhombic EPR and a very small *A*<sub>||</sub> of 15 × 10<sup>-4</sup> cm<sup>-1</sup> for the Cu-substituted, stable green form (Table 1). In addition, this species has a particularly strong absorbance at 459 nm with an  $\epsilon_1/\epsilon_2$  value of 1.0, indicative of a large tetrahedral distortion as in nitrite reductase. Both M121E and M121K-azurins at pH 3.5 as well as H80C-SOD(green) exhibit *A*<sub>||</sub> versus *g*<sub>||</sub> behavior (Figure 2) characteristic of T1 Cu sites.

**(b) Type 2 Copper Sites.** T2 sites are typified by tetragonal coordination of Cu(II) with four ligands that are either coplanar (Figure 1E) or slightly distorted from a coplanar array (Figure 1D). Although many T2 Cu complexes are known,<sup>19</sup> copper cysteine proteins in this category have only recently been created by site-directed mutagenesis and none has yet been characterized by X-ray crystallography. Characteristics of the

T2 sites in these proteins include an EPR *A*<sub>||</sub> > 90 × 10<sup>-4</sup> cm<sup>-1</sup> and a marked blue shift in the principal Cu-S absorption band ( $\lambda_1$ ) to ~410 nm (Table 1). A second, much weaker (Cys)S → Cu(II) CT band ( $\lambda_2$ ) may also be observed between 530 and 625 nm, which results in a large  $\epsilon_1/\epsilon_2$  value ≥ 1.8.

The azurin H117G mutant forms a T2 site in the presence of bidentate exogenous ligands such as histidine (Table 1).<sup>16</sup> The tetragonal character of this site, as evidenced by its EPR *A*<sub>||</sub> value of 156 × 10<sup>-4</sup> cm<sup>-1</sup>, is most likely achieved by addition of a fourth ligand (-NH<sub>2</sub>) to the (Im)<sub>2</sub>Cys plane. A similar T2 species is formed at pH 6 in the absence of added ligands, presumably by binding two H<sub>2</sub>O in place of the deleted His117 (Table 1). The T2 forms of H117G-azurin exhibit a linear relationship for *A*<sub>||</sub> versus *g*<sub>||</sub>, as shown by the upper line in Figure 2. The presence of a thiolate ligand causes this correlation line to appear at lower *A*<sub>||</sub> values than that for a series of T2 proteins lacking cysteine ligands.<sup>11,23,39</sup> Nevertheless, the EPR behavior of the T2 forms of H117G-azurin is distinctly different from T1 Cu sites and provides a standard for evaluating other T2 copper cysteine complexes such as those of the SOD mutants. The H46C and H120C mutants of the tetragonal Cu site in SOD<sup>18</sup> have their principal (Cys)S → Cu(II) CT band near 400 nm (Table 1) and *A*<sub>||</sub> versus *g*<sub>||</sub> behavior similar to the T2 azurin-H117G mutants (Figure 2). Similar T2 characteristics are observed for H80C(yellow) SOD, a short-lived intermediate formed initially upon addition of Cu to the tetrahedral Zn site.<sup>26</sup>

**(c) Type 1.5 Intermediate Cu Sites.** A different species is found for the M121K and M121E azurin mutants at pH 7.5 where the axial Lys and Glu ligands are deprotonated.<sup>24</sup> Their yellow color ( $\lambda_1$  = 410 and 417 nm, respectively) and high  $\epsilon_1/\epsilon_2$  values (> 1.8) place them in the T2 category (Table 1), but their *A*<sub>||</sub> versus *g*<sub>||</sub> values are far below the T2 azurin-H117G average (Figure 2). This suggests a geometry inbetween T1

(40) Petratos, K.; Dauter, Z.; Wilson, K. S. *Acta Crystallogr.* **1988**, *B44*, 628-636.

(41) Adman, E. T., personal communication.

**Table 2.** Resonance Raman Spectra of Copper(II) Cysteinate Proteins

sample <sup>a</sup>	RR frequencies (cm <sup>-1</sup> ) <sup>b</sup>													
	264	284	287	331	345	358	377	392	412	<b>430</b>	449	462	482	
type 1 axial Cu site														
amicyanin	264	284		331	345	358	377	392	412	<b>430</b>	449	462	482	
azurin	265	284	287		348		371	400	<b>408</b>	428	442	455	476	496
azurin-H117G (imidazole)	266	282			348		370	400	<b>406</b>	428	442	454	473	494
type 1 rhombic Cu site														
azurin-M121K (pH 3.5)	263	272			348	364	<b>371</b>	<b>404</b>	<b>407</b>	427		454	478	494
azurin-M121E (pH 3.5)	267	280			348		<b>370</b>	<b>399</b>	<b>408</b>	426	442	455	476	494
azurin-M121Q	259	275			351	361	<b>373</b>	<b>396</b>	<b>412</b>	429	446	460		
azurin-H46D	268	281	301	326	339		375	<b>400</b>	<b>410</b>	426	439	453	472	493
azurin-H117G (chloride)	260		301		347		<b>370</b>	<b>398</b>	407	429		457	482	494
SOD-Cu <sub>2</sub> Cu <sub>2</sub> H80C (green)	259	279			345	<b>355</b>		396	415					
type 1.5 intermediate Cu site														
azurin-M121K (pH 7.5)	266	275	302		<b>350</b>	<b>358</b>		397	416	430		454	476	
azurin-M121E (pH 7.5)	263		302	336	<b>343</b>	<b>356</b>		393		428				
SOD-Cu <sub>2</sub> Zn <sub>2</sub> H46C (pH 9.8)				332		<b>357</b>	373		407					
type 2 tetragonal Cu site														
SOD-Cu <sub>2</sub> Zn <sub>2</sub> H46C (pH 5.5)		271	298	320	<b>342</b>		378							
SOD-Cu <sub>2</sub> Zn <sub>2</sub> H120C		283			341	<b>359</b>	<b>366</b>	401						
SOD-Cu <sub>2</sub> Cu <sub>2</sub> H80C (yellow)		283	292	335	<b>348</b>			403						
azurin-H117G (histidine)	259		<b>296</b>	<b>319</b>	350			388		424				

<sup>a</sup> Proteins as in Table 1, except *P. aeruginosa* azurins: H117G with chloride as an exogenous ligand (ref 16) and H46D (refs 15 and 42). <sup>b</sup> RR spectra were obtained with 647.1-nm excitation for T1 sites (except azurin H46D for which 568.2 nm was used) and 413.1-nm excitation for T2 sites. Frequencies in boldface denote the most intense peak(s) in the spectrum.

and T2, as indicated by the dashed line in Figure 2 for a T1.5 intermediate Cu site. The T1.5 sites are likely to have more tetrahedral structures (Figure 1C) than T1 sites as a result of the replacement of the axial methionine with a stronger-binding fourth ligand. The pH 9.8 form of the H46C-SOD mutant also appears to be in the T1.5 intermediate category on the basis of its absorption and EPR behavior, possibly as a result of the addition of OH<sup>-</sup> as a ligand.

**Raman Spectroscopy as an Indicator of Cu-S Bond Length.** Resonance Raman spectroscopy provides detailed structural information on copper cysteinate sites. Excitation within a (Cys)S → Cu(II) CT band yields 4–12 fundamental vibrations in the 250–500-cm<sup>-1</sup> region (Table 2). The large number of frequencies compared to the single mode predicted for an isolated Cu-S center has been ascribed to kinematic and vibronic coupling of the Cu-S stretch with cysteine ligand deformations.<sup>13</sup> Proof for the dominant role of Cys comes from the fact that replacement of either the His or Met ligands of azurin has little effect on the RR spectrum. Thus, H46D-azurin,<sup>15</sup> H117G-azurin (chloride),<sup>16</sup> and M121E-azurin (pH 3.5) all have essentially the same set of Cu-Cys RR bands as wild-type azurin (Table 2). In contrast, replacement of the Cys ligand in C112D-azurin causes a complete loss of color and RR spectral properties.<sup>43</sup>

A similar type of enhancement of thiolate ligand vibrations has recently been observed in the RR spectra of Cu[HB(3,5-*i*Pr<sub>2</sub>pz)<sub>3</sub>]SR complexes,<sup>34</sup> the first model compounds to accurately reproduce the spectroscopic properties of T1 Cu sites (Table 1).<sup>31</sup> Replacement of the -SC(CH<sub>3</sub>)<sub>3</sub> ligand with -SCH(CH<sub>3</sub>)CH<sub>2</sub>CH<sub>3</sub> results in the splitting of the predominant ν(Cu-S) mode at 435 cm<sup>-1</sup> into three intense modes at 412, 432, and 446 cm<sup>-1</sup>. Normal coordinate analysis indicates that the splitting is due to kinematic coupling of the Cu-S stretch with S-C-C and C-C-C bends, as well as CH torsional motions, and that the degree of coupling is dependent on the conformation of the thiolate ligand.<sup>34</sup>

A comparison of RR spectra from different copper cysteinate proteins reveals a remarkably conserved set of frequencies for both the T1 and T2 sites (Table 2). These frequencies signify

a common set of internal vibrations of the cysteinate ligand which are enhanced via the (Cys)S → Cu(II) CT transition.<sup>6,9</sup> The uniqueness of each RR spectrum arises, instead, from variations in RR intensities (including the most intense band), and this parameter is sensitive to differences in the Cu-site geometry. Thus, in a progression from axial T1 to rhombic T1 to T2 sites, the same RR bands are observed but the maximum RR intensity (boldface numbers in Table 2) shifts from an average value of 420 cm<sup>-1</sup> for axial T1 to 390 cm<sup>-1</sup> for rhombic T1 and to 340 cm<sup>-1</sup> for T2 Cu sites. The two to three most intense features also tend to show substantial sulfur-isotope dependence,<sup>15</sup> indicating that the Cu-S stretch is undergoing kinematic coupling with cysteine fundamentals of similar energy. Thus, the shift of vibrational intensity to lower energy appears to be due to a lengthening of the Cu-S(Cys) bond. The use of the most intense RR features as an estimate of Cu-S bond strength has been discussed previously for T1 Cu proteins<sup>14</sup> and is analyzed in more detail below.

**Use of Isotopes to Identify the Cu-S Stretch.** (a) **Azurin-H117G (Imidazole).** The azurin H117G mutant (Figure 2) has been fully labeled with <sup>34</sup>S by growing bacteria on <sup>34</sup>S-sulfate. Although both Cys 112 and Met 121 are labeled, the failure of the Met 121 ligand to contribute to the RR spectrum<sup>16,44</sup> allows sulfur-isotope shifts to be ascribed to Cu-S(Cys) vibrations. Azurin-H117G reacted with exogenous imidazole has a RR spectrum essentially identical to wild-type azurin (Table 2).<sup>16</sup> In the <sup>34</sup>S-substituted protein (Figure 3A), four peaks exhibit isotope dependence (<sup>34</sup>S minus <sup>32</sup>S): the most intense peak at 406 (-2.0) cm<sup>-1</sup> and the adjacent peaks at 370 (-0.7), 400 (-1.4), and 428 (-1.2) cm<sup>-1</sup>. The total shift of 5.3 cm<sup>-1</sup> is close to the predicted shift of 7.7 cm<sup>-1</sup> for a pure Cu-S oscillator. These results are similar to those reported previously for wild-type azurin<sup>15</sup> where S-isotope shifts (<sup>34</sup>S minus <sup>32</sup>S) were observed at 409 (-3.8) and 428 (-1.4) cm<sup>-1</sup>, for a total shift of -5.2 cm<sup>-1</sup>. Hence, the ν(Cu-S) mode in the H117G-(Im) mutant is relatively localized and mainly mixes via kinematic coupling with δ(Cys) modes at 370, 400, 406, and 428 cm<sup>-1</sup>. The lack of detectable sulfur-isotope shifts for any of the other modes suggests that they have little Cu-S stretching character and, hence, gain intensity via vibronic coupling with the (Cys)S → Cu(II) CT transition.

(42) Germanas, J. P.; Di Bilio, A. J.; Gray, H. B.; Richards, J. H. *Biochemistry* **1993**, *32*, 7698–7702.

(43) Mizoguchi, T. J.; Di Bilio, A. J.; Gray, H. B.; Richards, J. H. *J. Am. Chem. Soc.* **1994**, *114*, 10076–10078.

(44) Thamann, T. J.; Frank, P.; Willis, L. J.; Loehr, T. M. *Proc. Natl. Acad. Sci. U.S.A.* **1982**, *79*, 6396–6400.

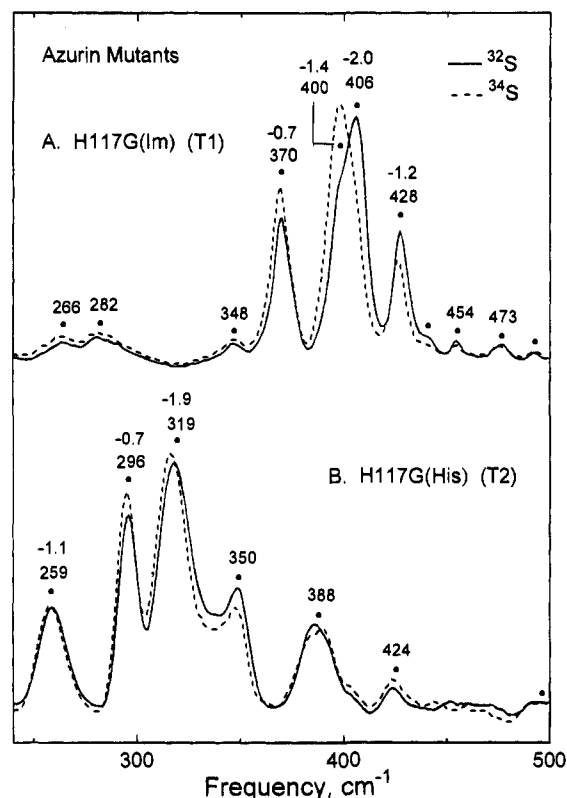


**Figure 3.** RR spectra of azurin-H117G substituted with  $^{32}\text{S}$  (—) or  $^{34}\text{S}$  (---) and reacted with 30 equiv of exogenous imidazole or histidine. (A) Azurin-H117G(Im): spectrum obtained on  $\sim 8$  mM protein at 15 K using 647.1-nm excitation (70 mW),  $4\text{-cm}^{-1}$  resolution, and 8 scans. (B) Azurin-H117G(His): spectrum obtained on 8 mM protein at 15 K using 413.1-nm excitation (40 mW),  $4\text{-cm}^{-1}$  resolution, and 6 scans. Peak frequencies are for the  $^{32}\text{S}$  samples with  $^{34}\text{S}$  shifts indicated above.

Copper-isotope substitution by reaction of apoprotein with  $^{63}\text{Cu}$  or  $^{65}\text{Cu}$  provides another means for identifying peaks with dominant Cu-ligand stretching character. However, the smaller change in the reduced mass of Cu relative to sulfur causes the shifts due to  $\nu(^*\text{Cu}-\text{S})$  to be only 25% of those observed for  $\nu(\text{Cu}-^*\text{S})$ . Reconstitution of azurin-H117G(Im) with  $^{65}\text{Cu}$  and  $^{63}\text{Cu}$  reveals isotope shifts at 283 ( $-1.7$ ), 370 ( $-0.7$ ), and 406 ( $-1.2$ )  $\text{cm}^{-1}$  (spectra not shown). The large shift of the low-frequency mode at 283  $\text{cm}^{-1}$  is consistent with its assignment as a Cu-N(His) stretch.<sup>13</sup> The Cu-isotope dependence of the 370- and 406- $\text{cm}^{-1}$  peaks is in good agreement with the S-isotope data and again shows that Cu-S(Cys) stretching character is limited to a few vibrational modes.

**(b) Azurin-H117G (Histidine).** Further evidence that RR peak intensity is related to  $\nu(\text{Cu}-\text{S})$  character comes from the behavior of azurin-H117G(His), a T2 species (Figure 2). In the RR spectrum of this protein (Figure 3B), maximum spectral intensity has become associated with vibrations that are  $\sim 100$   $\text{cm}^{-1}$  lower in energy than in the T1 species (Figure 3A). Maximum Raman intensity is again correlated with S-isotope dependence. In  $^{34}\text{S}$ -substituted azurin-H117G(His), the only three peaks showing significant S-isotope shifts ( $^{34}\text{S}$  minus  $^{32}\text{S}$ ) are the peaks at 259 ( $-1.1$ ), 296 ( $-0.7$ ), and 319 ( $-1.9$ )  $\text{cm}^{-1}$  (Figure 3B). Similarly, reconstitution of azurin-H117G(His) with Cu isotopes results in shifts ( $^{65}\text{Cu}$  minus  $^{63}\text{Cu}$ ) at 259 ( $-2.5$ ), 296 ( $-0.8$ ), and 319 ( $-0.5$ )  $\text{cm}^{-1}$  (spectra not shown). The  $\sim 100\text{-cm}^{-1}$  shift of RR intensity in this protein can be ascribed to a lengthening of the Cu-S(Cys) bond. The decreased force constant for the Cu-S stretch appears to favor kinematic coupling of  $\nu(\text{Cu}-\text{S})$  with lower frequency  $\delta(\text{Cys})$  modes (Table 2). The larger Cu- than S-isotope dependence at 259  $\text{cm}^{-1}$  is suggestive of a Cu-N(His) stretching component,

**Table 3.** Calculated Cu-S Distances in Copper Cysteinate Proteins

sample <sup>a</sup>	$\nu(\text{Cu}-\text{S})^b$	Cu-S(Cys) <sup>c</sup>
azurin	414	$\sim 2.13$
azurin-M121E (pH 3.5)	385	$\sim 2.16$
azurin-M121E (pH 7.5)	348	$\sim 2.21$
SOD-Cu <sub>2</sub> Cu <sub>2</sub> H80C (green)	351	$\sim 2.20$
SOD-Cu <sub>2</sub> Cu <sub>2</sub> H80C (yellow)	342	$\sim 2.22$
azurin-H117G (histidine)	298	$\sim 2.29$

<sup>a</sup> Proteins as in Table 1. <sup>b</sup> Weighted average of RR frequencies in  $\text{cm}^{-1}$  based on S-isotope dependence for WT azurin (ref 15) and azurin-H117G (Figure 3B), on Cu-isotope dependence of SOD-H80C (Figure 4), and on the two most intense peaks in azurin-M121E (Figure 7). <sup>c</sup> Cu-S distances in Å calculated by Badger's rule (ref 45) relative to the  $\sim 2.13\text{-Å}$  distance for WT azurin (refs 46 and 47).

and its decrease in energy relative to the 283- $\text{cm}^{-1}$  peak in T1 azurin-H117G(Im) can be ascribed to a lengthening of the Cu-N(His) bonds, as is expected for a tetragonal T2 species.

We have estimated the change in Cu-S(Cys) bond length between T1 azurin (wild-type) and T2 azurin-H117G(His) using Badger's rule.<sup>45</sup> A weighted average based on the S-isotope dependence yields a  $\nu(\text{Cu}-\text{S})$  value of 414  $\text{cm}^{-1}$  for wild-type azurin<sup>15</sup> and 298  $\text{cm}^{-1}$  for azurin-H117G(His). We assume that wild-type azurin has a Cu-S bond distance of  $\sim 2.13$  Å.<sup>46</sup> Thus, the 116- $\text{cm}^{-1}$  decrease in vibrational frequency corresponds to an  $\sim 0.16\text{-Å}$  increase in bond distance<sup>45</sup> and yields an estimated Cu-S bond of  $\sim 2.29$  Å in azurin-H117G(His) (Table 3). The latter value is well within the range of Cu-S bond distances observed for T2 Cu sites in model complexes.<sup>6,19</sup> The lengthening of the Cu-S(Cys) bond in azurin-H117G(His) is indicative of the presence of a fourth strong ligand in a tetragonal T2 site (Figure 1E).

**(c) SOD-H80C Mutants.** The slow conversion of the yellow to the green form of the H80C mutant of Cu<sub>2</sub>Cu<sub>2</sub>-SOD (Figure 2) is believed to be due to a conformational change (of the normally tetrahedral Zn site) from an initial tetragonal T2 structure (yellow) to a final rhombic T1 structure (green).<sup>26</sup> The RR spectra of these SOD species differ from those of azurins and other cupredoxins in that they tend to have a single dominant peak near 350  $\text{cm}^{-1}$  with three to four additional weak features between 250 and 450  $\text{cm}^{-1}$  (Figure 4). When the apoprotein is reconstituted with Cu isotopes, the only observed shifts ( $^{65}\text{Cu}$  minus  $^{63}\text{Cu}$ ) are in the intense bands at 348 ( $-1.0$ ) and 335 ( $-0.8$ )  $\text{cm}^{-1}$  in the yellow form (Figure 4A) or at 355 ( $-1.1$ ) and 345 ( $-0.7$ )  $\text{cm}^{-1}$  in the green form (Figure 4B). The Cu-isotope shifts strongly support the assignment of the  $\sim 350\text{-cm}^{-1}$  peak to the Cu-S(Cys) stretch in both H80C(yellow) and H80C(green) SOD. A Badger's rule analysis (Table 3) indicates a Cu-S bond length of  $\sim 2.22$  Å in H80C(yellow) and  $\sim 2.20$  Å in H80C(green). The similarity in Cu-S bond distances for these two SOD species is significant since H80C(yellow) has a broad EPR  $A_{\parallel}$  value of  $152 \times 10^{-4} \text{ cm}^{-1}$ , characteristic of a T2 site, whereas H80C(green) has a narrow EPR  $A_{\parallel}$  value of  $15 \times 10^{-4} \text{ cm}^{-1}$ , characteristic of a T1 site (Table 1). This observation suggests that, in contrast to a recent proposal,<sup>10</sup> the factors that lead to differences in EPR hyperfine splitting derive from differences in Cu coordination geometry rather than from differences in Cu-S(Cys) bond length.

(45) Herschbach, D. R.; Laurie, V. W. *J. Chem. Phys.* **1961**, *35*, 458–463. The change in bond distance,  $r$ , was calculated from the following relationship:  $(r_1 - d_{ij})/(r_2 - d_{ij}) = (\nu_2/\nu_1)^{2/3}$ . For a bond between S and a first-row transition metal,  $d_{ij}$  was estimated to be 1.5.

(46) Based on the X-ray crystallographic bond length of 2.13 Å for the Cu-S(Cys) in *A. denitrificans* azurin whose  $\nu(\text{Cu}-\text{S})$  of 411  $\text{cm}^{-1}$  (ref 35) is close to the 408- $\text{cm}^{-1}$  value for *P. aeruginosa* azurin. Structural studies of wild-type *P. aeruginosa* azurin reveal a Cu-S distance of 2.12 Å from EXAFS (ref 47), which is consistent with the above data, and a Cu-S distance of 2.25 Å from X-ray crystallography (ref 12), which is not.

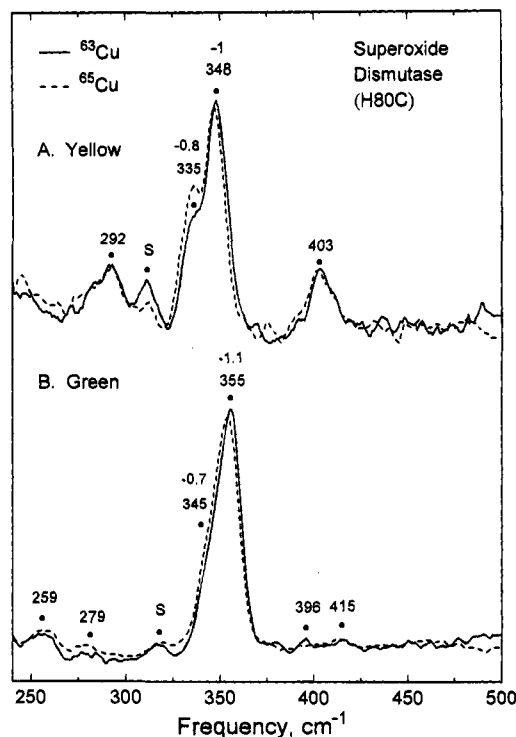


**Figure 4.** RR spectra of superoxide dismutase-H80C reconstituted with 4 equiv of  $^{63}\text{Cu}$  (—) or  $^{65}\text{Cu}$  (- - -). (A) Yellow form of H80C (2.5 mM in subunits) frozen within 1 min of Cu addition: spectra obtained at 90 K using 413.1-nm excitation (25 mW),  $7\text{-cm}^{-1}$  resolution, and accumulations of 13 and 14 scans for  $^{63}\text{Cu}$  and  $^{65}\text{Cu}$ , respectively. (B) Green form of H80C (2.5 mM) incubated 20 h at  $5^\circ\text{C}$  after Cu addition: spectra obtained at 15 K using 647.1-nm excitation (80 mW),  $5\text{-cm}^{-1}$  resolution, and accumulations of 16 and 9 scans for  $^{63}\text{Cu}$  and  $^{65}\text{Cu}$ , respectively. Peak frequencies are for the  $^{63}\text{Cu}$  samples with  $^{65}\text{Cu}$  shifts indicated above. S refers to a feature from the frozen solvent.

**Use of RR Intensity to Identify the Cu-S Stretch.** (a) **SOD-H46C and H120C.** The above studies on S- and Cu-isotope effects demonstrate that the bands with the greatest RR intensity are likely to have the greatest Cu-S stretching character, and thus provide information on Cu-S(Cys) bond length. The H46C (pH 5.5) and H120C mutants of CuZn-SOD are T2 species, based on their absorption and EPR properties (Table 1). Their RR spectra are dominated by  $\nu(\text{Cu-S})$  modes at 342 and  $366\text{ cm}^{-1}$ , respectively (Figure 5B,C), that are within the range for T2 sites (Table 1). The H46C mutant exhibits a change in EPR  $A_{\parallel}$  values with pH consistent with a distorted tetragonal T2 site at pH 5.5 and a T1.5 intermediate site at pH 9.8 (Figure 2). In addition, the RR spectrum exhibits a  $\nu(\text{Cu-S})$  of  $357\text{ cm}^{-1}$  at pH 9.8 (Figure 7A) compared to  $342\text{ cm}^{-1}$  at pH 5.5, which is indicative of a shortening of the Cu-S(Cys) bond in the pH 9.8 species. It is likely that the His 63 ligand which bridges the two metal sites of SOD at neutral pH has been displaced by a hydroxide ligand in H46C at pH 9.8, generating a more tetrahedral site.<sup>18b</sup> Nevertheless, when  $\nu(\text{Cu-S})$  falls within the  $340\text{--}365\text{-cm}^{-1}$  range, it is difficult to identify the exact coordination geometry by RR frequency alone (Figure 1).

(b) **Azurin-M121E and M121K.** At pH 3.5, the Glu and Lys axial ligands are protonated yielding structures with absorption and EPR parameters characteristic of rhombic T1 sites (Table 1). Their RR spectra are also typical of T1 sites (Figure 6A,B) with the enhanced intensity for the peaks at  $\sim 370$  and  $\sim 400\text{ cm}^{-1}$  being indicative of a rhombic distortion.<sup>16</sup> Deprotonation of the Glu and Lys ligands at pH 7.5 leads to T1.5 intermediate Cu sites based on EPR properties (Figure 2). In these species the maximum RR intensity has shifted to lower

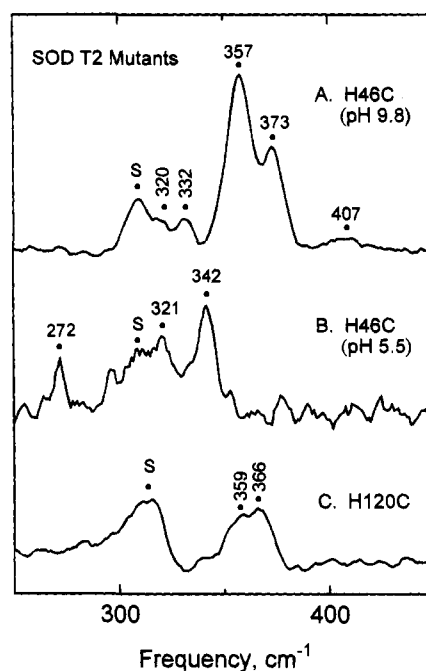


**Figure 5.** RR spectra of superoxide dismutase mutants. (A) H46C-(Cu<sub>2</sub>Zn<sub>2</sub>)SOD in pH 9.8 buffer containing 10 mM each of acetate, MES, HEPES, and TAPS: spectrum obtained on 2.5 mM protein at 15 K using 413.1-nm excitation (25 mW),  $7\text{-cm}^{-1}$  resolution, and 12 scans. (B) H46C-(Cu<sub>2</sub>Zn<sub>2</sub>)SOD in 0.1 M acetate (pH 5.5): spectrum obtained as in part C with 350.8-nm excitation (15 mW). (C) H120C-(Cu<sub>2</sub>Zn<sub>2</sub>)SOD in 0.1 M acetate (pH 5.5): spectrum obtained on 1.6 mM protein at 15 K using 406.7-nm excitation (20 mW),  $8\text{-cm}^{-1}$  spectral resolution, and 5 scans.

energy, yielding a pair of peaks at  $\sim 345$  and  $\sim 355\text{ cm}^{-1}$  (Figure 6C,D). The RR results imply a significant weakening of the Cu-S(Cys) bond due to the presence of a fourth strong ligand at pH 7.5 and, thus, are consistent with the T1.5 intermediate classification. Use of Badger's rule (Table 3) leads to calculated Cu-S(Cys) distances of  $\sim 2.16\text{ \AA}$  for M121E (pH 3.5) and  $\sim 2.21\text{ \AA}$  for M121E (pH 7.5), which are in excellent agreement with the EXAFS values of 2.15 and 2.21  $\text{\AA}$ , respectively.<sup>24c</sup> The Met121His axial-ligand mutants of azurin from *P. aeruginosa*<sup>48</sup> and *A. denitrificans*<sup>49</sup> have similar absorption EPR, and RR spectroscopic properties to M121E and M121K azurins, indicating that they also form a rhombic T1 site with protonated imidazole at low pH and a T1.5 intermediate site with deprotonated imidazole at neutral pH.

The T1.5 intermediate forms of the M121E and M121K azurin mutants at pH 7.5 exhibit two distinct absorption bands at  $\sim 415\text{ nm}$  and  $\sim 600\text{ nm}$  (Table 1, Figure 7). The more intense band at  $\sim 415\text{ nm}$  is in the expected energy range for the (Cys)S  $\rightarrow$  Cu(II) CT transition of a T1.5 or T2 site, and this assignment is verified by the observed enhancement of Cu-Cys vibrational modes with 413-nm excitation (Figure 6C,D). Excitation of either M121E or M121K within this  $\sim 600\text{-nm}$  absorption band produces the same vibrational frequencies as with 413-nm excitation, indicating that both of these absorption bands have substantial contributions from the same Cu-S(Cys) species. This behavior is documented in the excitation profile for M121E at pH 7.5 where the intensity of the  $343\text{-cm}^{-1}$   $\nu(\text{Cu-S})$  mode of the T1.5 component tracks both the 417- and 570-nm absorption bands (Figure 7).

(47) Murphy, L. M.; Strange, R. W.; Karlsson, B. G.; Lundberg, L.; Pascher, T.; Reinhammar, B.; Hasnain, S. S. *Biochemistry* **1993**, *32*, 1965-1975.

(48) Karlsson, B. G.; Bonander, N., unpublished results.

(49) Kroes, S. J.; Hoitink, C. W. G.; Canters, G. W. *J. Inorg. Biochem.* **1993**, *51*, 176.

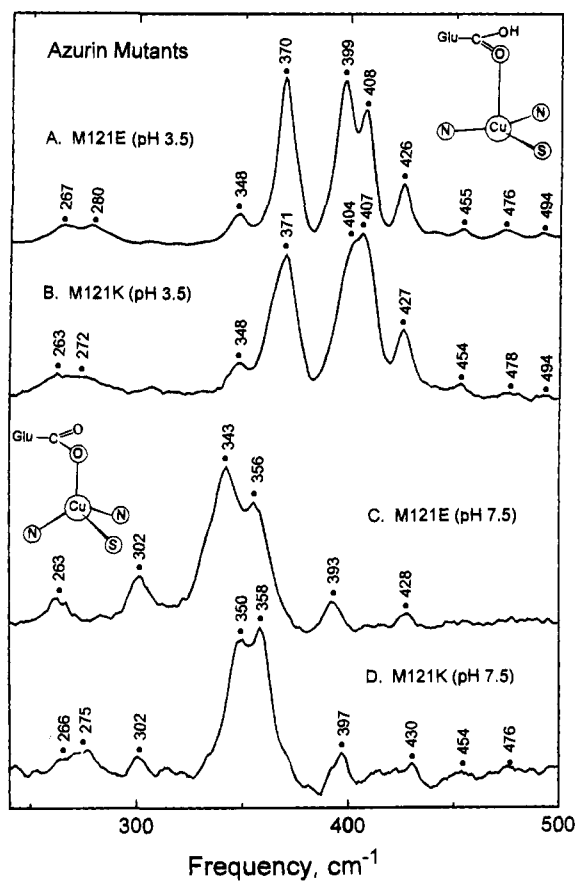


**Figure 6.** RR spectra of azurin-M121E and M121K mutants. (A) M121E in pH 3.5 buffer containing 10 mM HEPES: spectrum obtained on 6.3 mM protein at 15 K using 647.1-nm excitation (85 mW), 5-cm<sup>-1</sup> resolution, and 4 scans. (B) M121K (pH 3.5): spectrum obtained on 0.9 mM protein using 647.1-nm excitation (70 mW), 5-cm<sup>-1</sup> resolution, and 4 scans. (C) M121E in pH 7.5 buffer containing 10 mM HEPES: spectrum obtained on 5.5 mM protein at 15 K using 413.1-nm excitation (35 mW), 5-cm<sup>-1</sup> resolution, and 4 scans. (D) M121K (pH 7.5): spectrum obtained on 3.0 mM protein using 413.1-nm excitation (35 mW), 5-cm<sup>-1</sup> resolution, and 4 scans.

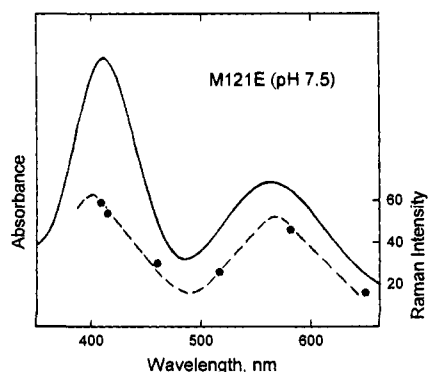


**Figure 7.** Absorption spectrum (—) and RR excitation profile (---) for the 343-cm<sup>-1</sup> mode of M121E-azurin (pH 7.5). Raman data were obtained using 5-cm<sup>-1</sup> resolution, as in Figure 6, but with a variety of excitation wavelengths. Peak heights were measured relative to the height of the 230-cm<sup>-1</sup> ice mode and converted to molar Raman intensities as described in Table 1.

The occurrence of two electronic transitions with substantial (Cys)S → Cu(II) CT character ( $\lambda_1$  and  $\lambda_2$  in Table 1) has previously been shown to be a common feature of T1 copper cysteine proteins.<sup>6,7</sup> For example, pseudoazurin and nitrite reductase exhibit RR enhancement of their  $\nu(\text{Cu-S})$  modes within both their ~450- and ~590-nm absorption bands.<sup>6</sup> The present work demonstrates that two (Cys)S → Cu CT transitions

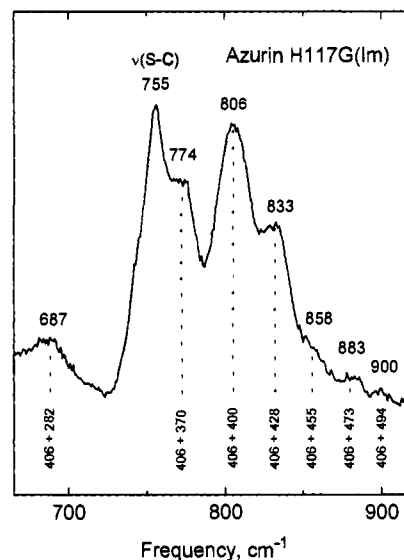


**Figure 8.** RR combination bands of azurin-H117G(Im). Spectrum obtained on 3.8 mM protein at 15 K using 647.1-nm excitation (120 mW), 7-cm<sup>-1</sup> resolution, and 4 scans. Combination bands are identified below by the sum of their constituent fundamental frequencies. The fundamental at 755 cm<sup>-1</sup> is assigned to the S-C stretch of cysteine.

are also common for T1.5 copper cysteine proteins, as in azurin-M121E and M121K at pH 7.5 and SOD-H46C at pH 9.8 (Table 1). Similarly, the Raman excitation profile for the T2 tetragonal H80C (yellow) form of SOD shows enhancement of its 348-cm<sup>-1</sup>  $\nu(\text{Cu-S})$  mode within both the 411- and 604-nm absorption bands.<sup>26</sup> Based on the electronic spectral analyses of Solomon and co-workers,<sup>5,7</sup> the intense ~410-nm absorption of T1.5 and T2 Cu sites is expected to have contributions from cysteine S p and Cu d orbitals with  $\sigma$  overlap, whereas the weaker ~580-nm absorption of T2 Cu sites is more likely to arise from S and Cu orbitals with  $\pi$  overlap.

**Use of Combination Bands to Identify the Cu-S Stretch in T1 Sites.** Previous RR studies of T1 Cu proteins have noted the large number of combination bands between 700 and 900 cm<sup>-1</sup> arising from the sum of copper cysteine fundamentals in the 250–500 cm<sup>-1</sup> region.<sup>13,14</sup> All of the T1 Cu proteins in the present study also exhibit a set of combination bands. For example, H117G azurin reconstituted with exogenous imidazole has a cysteine sulfur-carbon stretching fundamental at 755 cm<sup>-1</sup>, with all other vibrational modes between 650 and 900 cm<sup>-1</sup> being assignable as combination bands (Figure 8). A remarkable and apparently universally applicable aspect of these combination bands is that they are mainly generated by a *single* fundamental, referred to here as  $\nu_c$ . In the case of H117G(Im), it is the predominant  $\nu(\text{Cu-S})$  mode at 406 cm<sup>-1</sup> which serves as  $\nu_c$  and adds with most of the other cysteine fundamentals (Figure 3A, Table 2) to produce the observed combination bands (Figure 8). Table 4 shows a similar behavior for a number of other axial and rhombic T1 Cu proteins including amicyanin, pseudoazurin, and nitrite reductase. In each case in Table 4, the observed combination frequencies (shown in *italics*) can be obtained by taking the unique value of  $\nu_c$  for each protein and summing it with the other observed RR fundamentals. A similar identification of  $\nu_c$  has been made for the T1 mutants of azurin-M121 and SOD-H80C and the Cu(pz)<sub>3</sub>(S-*t*Bu) model complex (Table 1). In addition, we note that the previously reported combination bands of plastocyanin, stellacyanin, and laccase<sup>13,14</sup> can also be accounted for in each case by a single  $\nu_c$  at 425, 387, and 383 cm<sup>-1</sup>, respectively.

It is striking that  $\nu_c$ , the generator of combination bands, generally corresponds to the most intense band in the RR spectrum (Table 1) and, therefore, serves as another indicator



**Table 4.** Combination Bands Generated by  $\nu_c$  plus other Copper-Cysteinate Fundamentals<sup>a</sup>

protein	RR frequencies of <b>observed combination bands</b> and contributing fundamentals							
	$\nu_c$	$\nu_c + \nu_1$	$\nu_c + \nu_2$	$\nu_c + \nu_3$	$\nu_c + \nu_4$	$\nu_c + \nu_5$	$\nu_c + \nu_6$	$\nu_c + \nu_7$
T1 axial Cu site								
amicyanin	768	807	820	842	859	894	911	
$\nu_c = 430$	345	377	392	412	430	462	482	
azurin-H117G (imidazole) <sup>b</sup>	687	774		806	833	858	883	900
$\nu_c = 406$	282	370		400	428	454	473	494
T1 rhombic Cu site								
azurin-M121E (pH 3.5)	661	682	744	768	800	806		
$\nu_c = 399$	267	280	348	370	399	408		
pseudoazurin			726		766	781	831	
$\nu_c = 385$		339		385	397	416	445	
nitrite reductase			723		761	774	795	833
$\nu_c = 364$			364		397	411	431	471

<sup>a</sup>  $\nu_c$  = frequency of RR fundamental (in  $\text{cm}^{-1}$ ) that generates **combination bands** by summation with other fundamentals. Observed combination bands occur at slightly lower frequency than the sum of the constituent fundamentals due to the anharmonicity of the vibrational potential well. Proteins and RR spectra as in Tables 1 and 2. <sup>b</sup> Similar combination bands are observed for wild-type azurins from *P. aeruginosa* (ref 14) and *A. denitrificans* (ref 35) based on  $\nu_c$  values of 408 and 411  $\text{cm}^{-1}$ , respectively.

of the mode with the greatest Cu-S(Cys) stretching character. Furthermore, in cases where the RR spectrum has several intense features, the  $\nu_c$  frequency may actually provide the best means of determining  $\nu(\text{Cu-S})$ . This can be seen, for example, in the T1 form of azurin-M121E at pH 3.5 which has equally intense fundamentals at 370 and 399  $\text{cm}^{-1}$  (Figure 6A), but only the 399- $\text{cm}^{-1}$  mode gives rise to combination bands (Table 4). The tendency of a single fundamental to generate the majority of the combination bands has been noted previously for the 408- $\text{cm}^{-1}$  mode of wild-type azurin and has been ascribed to the large excited-state Duschinsky mixing of modes involving the Cu-S stretch.<sup>14</sup>

**RR Frequencies and Coordination Geometry.** The present study shows that RR spectroscopy can identify the Cu-S(Cys) stretching frequency by (i) its large S- or Cu-isotope shift, (ii) its high RR intensity, and (iii) its role as the principal generator of combination bands. We propose that the energy of the  $\nu(\text{Cu-S})$  mode is strongly related to the geometry of the Cu site (Table 1). The following ranges for  $\nu(\text{Cu-S})$  are observed: 430–405  $\text{cm}^{-1}$  for T1 axial (Figure 1A), 405–355  $\text{cm}^{-1}$  for T1 rhombic (Figure 1B), 360–340  $\text{cm}^{-1}$  for T1.5 intermediate (Figure 1C), 365–340  $\text{cm}^{-1}$  for T2 distorted tetragonal (Figure 1D), and 320–300  $\text{cm}^{-1}$  for T2 tetragonal (Figure 1E). The trend in  $\nu(\text{Cu-S})$  values with T1 axial > T1 rhombic > T2, is indicative of an increase in Cu-S(Cys) bond length from  $\sim 2.13$  Å in T1 axial to  $\sim 2.29$  Å in T2 tetragonal, by application of Badger's rule.<sup>43</sup> The progressive weakening of the Cu-S(Cys) bond can be explained by increased electron density on the Cu ion arising from increased interaction with a fourth ligand (Figure 1). The proposed trend in Cu-S bond strengths is further supported by the energy of the sulfur-carbon stretch of cysteine which increases as  $\nu(\text{Cu-S})$  decreases. Thus,  $\nu(\text{S-C})$  values range from  $\sim 755$   $\text{cm}^{-1}$  for T1 axial to 760–770  $\text{cm}^{-1}$  for T1 rhombic and 765–775  $\text{cm}^{-1}$  for T1.5 and T2 (Table 1).

In the progression from T1 axial to T1 rhombic Cu sites, the increased influence of the fourth ligand is manifested in the movement of the Cu ion toward the axial position, creating a tetrahedral distortion of the trigonal plane (Figure 1A,B). Previous studies of T1 Cu sites<sup>6,7</sup> have indicated that the ratio of absorption intensities,  $\epsilon_1/\epsilon_2$  (Table 1), increases with the degree of rhombic distortion (going from trigonal towards tetrahedral geometry) and correlates with an increased strength of the axial ligand bond in X-ray crystal structures. Thus,  $\epsilon_1/\epsilon_2$  varies from  $\sim 0.1$  for axial T1 sites to  $\sim 1.0$  for highly rhombic T1 sites, with corresponding Cu-S(Met) distances of  $\sim 2.9$  and  $\sim 2.6$  Å, respectively. We now note that  $\nu(\text{Cu-S})$  and, in particular,  $\nu_c$ , the mode that generates combination bands, shows an excellent correlation with  $\epsilon_1/\epsilon_2$  (Figure 9). As the rhombic distortion increases on going from amicyanin to nitrite reductase,

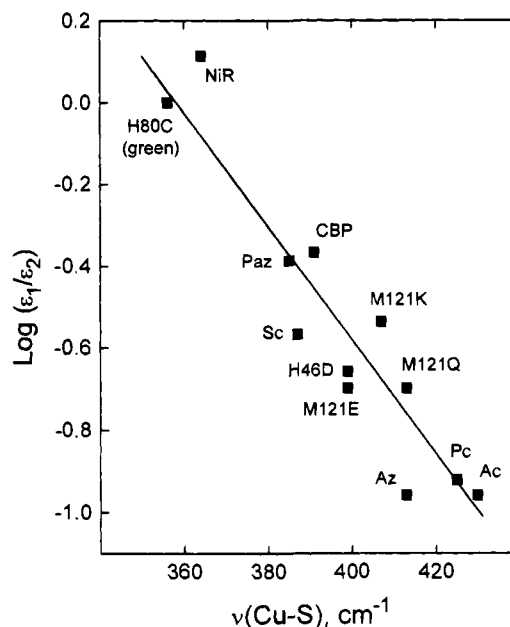


**Figure 9.** Correlation of the Cu-S(Cys) stretching frequency with the  $\epsilon_1/\epsilon_2$  absorbance ratio for T1 Cu sites. Proteins included are amicyanin (Ac), azurin-H46D, SOD-Cu<sub>2</sub>Cu<sub>2</sub>-H80C (green), azurin-M121E (pH 3.5), azurin-M121K (pH 3.5), azurin-M121Q, cucumber basic protein (CBP), nitrite reductase (NIR), pseudoazurin (Paz), plastocyanin (Pc), and stellacyanin (Sc). Data from Tables 1–3 except for spinach Pc (refs 6 and 14), CBP (refs 6 and 9), and *Rhus vernicifera* Sc (refs 6 and 13). The  $\nu(\text{Cu-S})$  in each case is  $\nu_c$ , the frequency that generates the combination bands.

the vibrational frequency of the dominant Cu-S stretching mode decreases. This lengthening of the Cu-S(Cys) bond is expected as the Cu moves out of the trigonal His<sub>2</sub>Cys ligand plane and toward the weaker axial ligand. The frequency change in  $\nu(\text{Cu-S})$  from 408  $\text{cm}^{-1}$  in azurin to 364  $\text{cm}^{-1}$  in nitrite reductase would correspond to a Cu-S(Cys) bond lengthening of  $\sim 0.05$  Å (from  $\sim 2.13$  to  $\sim 2.18$  Å) according to Badger's rule.<sup>45</sup> Such a change in bond length is more readily detected by RR spectroscopy than by X-ray crystallography where it lies within the  $\pm 0.07$  Å error range for metal-ligand bond distances.<sup>17</sup>

It is of interest that azurin with its  $\nu(\text{Cu-S})$  at 408  $\text{cm}^{-1}$  has a weaker Cu-S bond than plastocyanin whose predominant  $\nu(\text{Cu-S})$  occurs at 422  $\text{cm}^{-1}$  according to its S-isotope dependence.<sup>50</sup> Yet a similar trigonal planar character for these two proteins is indicated by their  $\epsilon_1/\epsilon_2$  ratios (Figure 9) as well as their X-ray structures.<sup>8</sup> The difference in Cu-S bond strength may well be due to the presence of a weak fifth axial carbonyl

(50) Qiu, D.; Hecht, M. H.; Spiro, T. G., personal communication.

ligand in the crystal structure of azurin which is not present in any other T1 Cu protein.<sup>8</sup>

A further distortion of the T1 rhombic site occurs as the strength of the axial ligand increases. Deprotonation of the axial ligands of the M121E and M121K azurin mutants leads to a T1.5 intermediate Cu site (Figure 1C) whose  $\nu(\text{Cu-S})$  values are  $\sim 50 \text{ cm}^{-1}$  lower than in the corresponding T1 protonated forms (Figure 6). The formation of a T2 tetragonal site (Figure 1E) as in the H117G azurin mutant with exogenous histidine results in an even lower energy of  $\sim 320 \text{ cm}^{-1}$  for  $\nu(\text{Cu-S})$ , a drop of another  $30 \text{ cm}^{-1}$ . This difference most likely relates to the location of the amino acid substitution within the Cu coordination sphere. The H117G mutation results in the removal of a ligand from the NNS ligand plane whereas the Met 121 mutations leave the NNS ligand plane intact. It appears that the copper site in the H117G mutant is sufficiently flexible to add two ligands to the Cu-NS plane to generate a T2 tetragonal site.

**RR Intensities and Coordination Geometry.** Vibronic and kinematic coupling are two mechanisms by which Raman modes can undergo resonance intensity enhancement and which help to account for the large number of vibrational modes in the RR spectra of copper cysteine proteins. Displacement of atoms along the Cu-S coordinate in the electronic excited state (involving  $\text{S} \rightarrow \text{Cu CT}$ ) is responsible for  $\nu(\text{Cu-S})$  being the most intense feature in the RR spectrum.<sup>14</sup> A large number of other fundamental vibrations of the cysteine moiety (such as the S-C stretch) occur between 250 and  $1500 \text{ cm}^{-1}$  with similar intensities for T1 and T2 Cu sites.<sup>51</sup> These most likely arise via extended *vibronic coupling* such that all of the atoms of the cysteine moiety undergo displacements in the electronic excited state. Additional intensity enhancement occurs by ground-state *kinematic coupling* of the Cu-S stretch with cysteine fundamentals of similar energy. Such kinematic coupling is believed to be favored by the coplanar character of the  $\text{Cu-S}_\gamma\text{-C}_\beta\text{-C}_\alpha\text{-N}$  moiety,<sup>13</sup> a highly conserved structural feature in many T1 proteins of known structure.<sup>9</sup>

Axial and rhombic T1 sites typically exhibit three to four strongly enhanced modes which arise from kinematic coupling of  $\nu(\text{Cu-S})$  with  $\delta(\text{Cys})$  modes of similar energy.<sup>9</sup> Examples are the four peaks between 370 and  $428 \text{ cm}^{-1}$  for the T1 axial site of H117G(Im) azurin (Figure 3A) and for the T1 rhombic site of M121E and M121K azurins (Figure 6A,B). An approximate measure of Raman enhancement can be obtained by calculating the intensity of the mode with the most  $\nu(\text{Cu-S})$  character relative to that of the ice mode and normalizing to a sulfate standard (*I* values in Table 1). Such calculations involve considerable error ( $\pm 30\%$ ), in part because it is frequently not possible to obtain data at the maximum enhancement wavelength. Nevertheless, it can be seen that T1 axial sites have the greatest enhancements, with relative Raman intensities of 500–750 (Table 1). T1 rhombic sites with  $\nu(\text{Cu-S})$  below  $400 \text{ cm}^{-1}$  exhibit weaker relative Raman intensities of only 130–360.

T1.5 intermediate and T2 tetragonal sites show the weakest kinematic coupling with relative Raman intensities for  $\nu(\text{Cu-S})$  of 15–150 (Table 1). Model copper(II) thiolate complexes with T2 tetragonal sites<sup>6</sup> show similarly weak relative Raman intensities of 10–60. As in the case of  $\nu(\text{Cu-S})$  frequencies, there is some overlap between the Raman intensities for T1 rhombic and T1.5 intermediate sites, making it difficult to

distinguish these two geometries by RR spectroscopy. However, the T1.5 and T2 sites do appear to differ from the T1 rhombic sites in their lack of combination bands (Table 1), even when relative Raman intensities are as high as 150. The loss of combination bands may be related to a change in the orientation of Cu and S molecular orbitals in T1.5 and T2 sites which lessens the probability for Duschinsky mixing.<sup>14</sup> The change in orbital orientation has been extensively investigated in order to explain the observed differences in their  $(\text{Cys})\text{S} \rightarrow \text{Cu(II)}$  electronic transitions.<sup>5,7</sup> In general, T1 Cu sites have their greatest absorption intensity associated with  $\lambda_2$  at  $\sim 600 \text{ nm}$  whereas T2 Cu sites have their greatest absorption intensity associated with  $\lambda_1$  at  $\sim 410 \text{ nm}$  (Table 1).

## Conclusions

1. All of the copper cysteine proteins studied, regardless of coordination geometry, show multiple RR bands due to coupling of  $\nu(\text{Cu-S})$  with internal vibrations of the cysteine ligand. Such coupling is also observed in the RR spectra of iron cysteine proteins such as ferredoxin and HiPIP,<sup>52</sup> but their cysteine ligand contributions are far less extensive than in the copper proteins.

2. Sulfur- and copper-isotope substitution shows that  $\nu(\text{Cu-S})$  correlates with the most intense peak in the RR spectrum. This is also the peak that generates combination bands.

3. For T1 Cu sites,  $\nu(\text{Cu-S})$  frequencies range from 430 to  $405 \text{ cm}^{-1}$  for axial and from 405 to  $355 \text{ cm}^{-1}$  for rhombic geometries, indicating a gradual decrease in Cu-S(Cys) bond strength with increasing rhombicity. The lengthening of the Cu-S(Cys) bond, due to movement of Cu from the equatorial ligand plane toward the weaker axial ligand, also correlates with an increase in the absorbance ratio ( $\epsilon_{460}/\epsilon_{600}$ ) which varies from 0.1 for axial to 1.3 for highly rhombic T1 sites.

4. The  $\nu(\text{Cu-S})$  frequencies range from 365 to  $340 \text{ cm}^{-1}$  for T1.5 intermediate and T2 distorted tetragonal sites and from 320 to  $300 \text{ cm}^{-1}$  for sites closer to square planar. The lower frequencies of these sites indicate a further lengthening of the Cu-S(Cys) bond when there are four strong ligands. The T2 geometry is also characterized by higher energy and increased intensity for the  $\sim 410\text{-nm}$   $(\text{Cys})\text{S} \rightarrow \text{Cu(II)}$  CT band, leading to absorbance ratios ( $\epsilon_{410}/\epsilon_{580}$ ) of 1.9 to 3.3.

5. Copper sites in copper cysteine proteins are clearly capable of existing in a continuum of structures with the geometry being determined by the location of the two to three other strong ligands in addition to cysteine.

**Acknowledgment.** We are grateful to Dr. Jane Han for helpful discussions and assistance in obtaining RR spectra. We thank Dr. Erik Vijgenboom for aiding in the preparation of <sup>34</sup>S-azurin-H117G. We also thank Drs. Roman Czernuszewicz and Thomas G. Spiro for making data available prior to publication. This research was supported by the National Institutes of Health, Grants GM 18865 (T.M.L., J.S.-L.) and GM 28222 (J.S.V.), the Swedish National Science Research Council (B.G.K.), the STW Technology Foundation of the Department of Economic Affairs of The Netherlands (G.W.C.), and the North Atlantic Treaty Organization, Grant RG 930170 (T.M.L., G.W.C.).

(52) (a) Han, S.; Czernuszewicz, R. S.; Spiro, T. G. *J. Am. Chem. Soc.* **1989**, *111*, 3496–3504. (b) Backes, G.; Mino, Y.; Loehr, T. M.; Meyer, T. E.; Cusanovich, M. A.; Sweeney, W. V.; Adman, E. T.; Sanders-Loehr, J. *J. Am. Chem. Soc.* **1991**, *113*, 2055–2064.

(51) Andrew, C. R.; Sanders-Loehr, J., unpublished results.